UNIZIK JOURNAL OF ENGINEERING AND APPLIED SCIENCES (UJEAS)

Research Article

Effect of projectile shape on laminate composite materials (mild steel-bulk metallic glass-dyneema) as ballistic protection using computational analysis

Orueri D. U, Akindap J. O, Johnson-Anamemena N, Hassan N

Special Issue
A Themed Issue in Honour of Professor Ekedimogu Eugene Nnuka on His retirement.

This themed issue honors Professor Ekedimogu Eugene Nnuka, celebrating his distinguished career upon his retirement. His legacy of exemplary scholarship, mentorship, and commitment to advancing knowledge is commemorated in this collection of works.

Edited by
Chinonso Hubert Achebe PhD.
Christian Emeka Okafor PhD.

UJEAS

UNIZIK JOURNAL OF ENGINEERING AND APPLIED SCIENCES

UNIZIK Journal of Engineering and Applied Sciences 3(2), June (2024), 620-630
Journal homepage: https://journals.unizik.edu.ng/index.php/ujeas
PRINT ISSN: 2992-4383 || ONLINE ISSN: 2992-4391

Effect of projectile shape on laminate composite materials (mild steel-bulk metallic glass-dyneema) as ballistic protection using computational analysis

Orueri D. U[1*], Akindap J. O[1], Johnson-Anamemena N[2]. and Hassan N[3]
[1]Mechanical Engineering Department, Nigerian Defence Academy, Kaduna
[2]Mechanical Engineering Department, Air Force Institute of Technology, Kaduna
[3]Aerospace Engineering Department, Air Force Institute of Technology, Kaduna
[*]Corresponding Author's E-mail: danieldakseal@gmail.com

Abstract
This study investigated the influence of projectile geometry on the ballistic performance of laminate composite materials for protective systems. Advanced computational analysis using Abaqus Explicit FEA software compared two projectile configurations, blunt-nose and conical, against laminate materials including mild steel, Bulk metallic glass, and Dyneema, with a 9 mm plate thickness target. The study reveals that over a velocity range of 215 m/s to 275 m/s, the conical projectile induces significantly higher Von Mises stress levels compared to the blunt-nose projectile. This effect is attributed to the conical projectile's piercing action causing localized plastic strain and petal-like formations, while the blunt projectile results in plug ejection from the target material. The research highlights the complex failure mechanisms associated with different projectile geometries, with the conical projectile inducing radial necking and petalling, and the blunt projectile causing indentations and plug ejection. These findings underscore the reproducibility of established trends and contribute to understanding the ballistic behavior of laminate composite materials.

Keywords: Blunt; Bulk Metallic Glass; Conical; Deformation; Dyneema; Mild Steel; Von Mises stresses.

1. Introduction

Small-arms projectiles are prevalent in conflicts worldwide due to their affordability and ease of use, necessitating effective protection against them. Various materials, including metal alloys, ceramics, polymers, and composites, are crucial for structural protection technology. The ballistic resistance of armor plates depends on factors such as material properties, thickness, angle of impact, and projectile shape and size (Senthil *et al*., 2017a; Senthil *et al*., 2017c). Recent studies have highlighted the importance of projectile nose shape in determining armor plate resistance. For instance, ogive-shaped projectiles exhibit higher ballistic limits compared to blunt ones. Additionally, the method of plate production, such as additive manufacturing, can impact ballistic performance. Finite Element Method (FEM) simulations have been instrumental in understanding the ballistic behavior of materials like aluminum alloys and lattice structures (Orueri *et al*., 2023).

Naik *et al* (2024) conducted a numerical study using LS-Dyna to investigate the impact of different projectile nose shapes on a 5 mm thin target plate. They found that ogive-shaped projectiles demonstrated the highest ballistic limit, while blunt projectiles exhibited the lowest. The impact phenomena varied among nose shapes, with plugging failure observed for blunt projectiles, plug and small fragment formation for hemispherical projectiles, radial necking and fragmenting failure for conical projectiles, and petal formation for ogive projectiles. Kristoffersen *et al* (2020) compared the ballistic perforation resistance of additively manufactured aluminum plates with traditionally die-cast ones. They found negligible performance differences between the two, suggesting that additively produced materials may possess equal or superior ballistic qualities.

Nirmal *et al* (2021) utilized FEM simulations to explore the impact behavior of additively made AlSi10Mg alloy and its ballistic limit against different projectiles. They observed plugging and petaling failure for hemispherical projectiles and plugging failure for blunt projectiles, with hemispherical projectiles exhibiting a higher ballistic limit. Oktay *et al* (2022) investigated the ballistic performance of body-centered lattice structures with varying cell heights. They discovered that increasing the aspect ratio of the unit cell improved penetration resistance, and optimizing the unit cell height enhanced the ballistic performance of lattice structures.

Tiwari *et al* (2017) examined the influence of projectile nose shape, target span, and boundary condition on the ballistic limit of thin aluminum plates. Their study revealed significant effects of target span and boundary fixity on the ballistic limit, with an increase in target span diameter leading to an increase in ballistic limit and the opposite trend observed with an increase in fixity region. Khaire *et al* (2020) conducted finite element investigations to analyze the performance of 1 mm thick aluminum alloy hemispherical shell targets struck by ogive nose projectiles. They found that the ballistic limit was highest for aluminum alloy Al-7075 among the alloys studied. Yang and Chen (2017) aimed to identify the ballistic characteristics of UHMWPE UD laminate for hybrid soft body armor design. They found that thermal damage of UHMWPE fibers during ballistic impact degraded material properties, resulting in decreased ballistic performance, particularly when Dyneema UD laminate was placed on the striking face before Twaron fabric.

Senthil *et al* (2017a) conducted numerical investigations on 2024 aluminum alloy plates against cylindro-conical hardened steel projectiles using ABAQUS finite element code. The study focused on the ballistic resistance of targets with an initial obliquity of 40° against 60° cylindro-conical nose projectiles, comparing results with available experimental data. ABAQUS/Explicit, coupled with the Johnson-Cook elasto-viscoplastic material model, was employed for simulations. The simulations accurately predicted the formation of petals, velocity drop, and target deformation against conical projectiles, aligning well with experimental findings. In their study, Senthil *et al* (2017b) conducted an investigation into the ballistic response of 2024 aluminum plates when subjected to impact by a blunt nose projectile. The researchers employed Finite Element Method (FEM) simulation using Abaqus FEA software to anticipate the material response upon encountering the blunt projectile. The numerical findings exhibited a high degree of agreement with experimental observations. Analysis of the target's failure mode revealed the formation of cracks shaped like plugs, with each plug exhibiting a diameter equivalent to that of the projectile across all observed targets.

The aim of this research is to explore the impact of projectile shape, particularly comparing the effects of blunt and conical projectiles. Using advanced computational analysis facilitated by Abaqus Explicit FEA software, the study delves into the interaction dynamics between mild steel, Bulk metallic glass, and Dyneema. This laminate system of ballistic protection was proposed by the author in another paper due to its exceptional ballistic limit (Akindapo *et al*., 2023). Hence, very limited literature exists for the characterization and behaviour of the laminate target against various projectile nose shapes to study the effect for those of a conical 7.62 mm API projectile and its blunt-faced counterpart.

1.1 Governing Equations for the Simulation

The various governing equations used are discussed below;

The constitutive model earlier derived and used by the same author on modeling and simulation of laminate composite materials for use as ballistic protection was employed in this work (Orueri, 2023).

1.2 One-Dimensional Model for Fabric Armour

1. Introduction

Imagine pulling a string from one end while the other end stays put. Two types of waves travel along the string: one moves back and forth along the string, while the other spreads out like a fan.

2. Three Regions of Interest

i. First Region: Before the waves start, the string is still.

ii. Second Region: As the waves move, the string stretches but stays horizontal.

iii. Third Region: At the end, the string moves vertically.

3. Key Equation

The main equation relates the stress on the string to its movement:

$$\sigma = \rho \ddot{R} \qquad (1)$$

This tells us how the stress (σ) on the string relates to its movement (¨R¨), with ρ representing density.

4. Wave Speeds

The speed of the waves depends on the material of the string and its density (Akindapo *et al*., 2023):

$$c = \sqrt{\frac{E}{\rho}}\,,\ \ D = c\left[\sqrt{\varepsilon(1+\varepsilon)} - \varepsilon\right] \qquad (2)$$

$$\sigma = \rho c^2 \varepsilon,\ Q = 2A\sigma sin\alpha = 2A\rho cv(\left[\sqrt{\varepsilon(1+\varepsilon)} - \varepsilon\right]^2 + \frac{v^2}{c^2})^{-\frac{1}{2}} \qquad (3)$$

Here, c is the speed of the waves, D is another wave speed, E is a material property called modulus, and ε represents strain.

5. Strength Conditions

We want to know how much force the string can handle before breaking. This depends on the speed of the waves and the material properties:

$$Q = 2^{\frac{2}{3}} A E^{\frac{1}{6}} \rho^{\frac{5}{6}} v^{\frac{5}{3}} < B\sigma^{**} \qquad (4)$$

And $\sigma = 2^{-\frac{1}{3}} E^{\frac{1}{3}} \rho^{\frac{1}{3}} v^{\frac{4}{3}} < \sigma^{*}$ (5)

Here, Q is the force, A is a cross-sectional area, B is the impact area, σ∗ is a limiting stress, and σ∗∗ is another limiting stress (Akindapo *et al*., 2023).

6. Bullet Impact

When a bullet hits the string, its motion is influenced by the force applied by the string:

$$m\frac{dv}{dt} = B\sigma^{**}\left(\frac{v}{v_o}\right)^{\frac{5}{3}} \qquad (6)$$

This equation describes how the velocity (v) of the bullet changes over time (t), influenced by its mass (m), initial velocity (v_o), and the force (Bσ∗∗) applied by the string.

7. Simplified Axisymmetric Formulation

If we simplify things further by considering a circular fabric instead of a string, we can still understand how it behaves when subjected to stress and when a bullet hits it.

8. Contact Condition

When the bullet hits the fabric, we want to know how it affects the fabric's shape:

$$w(r_o, t) = W(t) \qquad (7)$$

Here, w is the displacement, r_o is the radius of the bullet, and W is the shape of the fabric (Akindapo *et al*., 2023).

2.0 Material and methods

The following materials were used in this research work;

Mild steel, Bulk metallic glass, Dyneema and 7.62 mm API Projectile. The design properties employed for the mild steel target and projectile are shown in Table 1 below;

Table 1: Material Properties for Mild steel target and projectile (Senthil *et al.*, 2017; Guodong *et al.*, 2020)

Description	**Mild steel (Projectile)**	**Mild steel (Target)**
Modulus of elasticity	210×10^9 N/m^2	203×10^9 N/m^2
Poisson’s ratio, υ	0.3	0.33
Density	7850 Kg/m^3	7850 Kg/m^3
Yield stress constant, A	0.95×10^9 N/m^2	304.330×10^6 N/m^2
Strain hardening constant, B	0.725×10^9 N/m^2	422.007×10^6 N/m^2
N	0.375	0.345
Viscous effect, C	0.015	0.0156
Thermal softening constant, M	0.625	0.87
Reference strain rate, έo	1 s-1	0.0001 s^{-1}
Melting temperature	1793 K	1800 K
Transition temperature	293 K	293 K
Fraction strain constant, D1	-0.8	0.1152
D2	2.1	1.0116
D3	0.5	-1.7684
D4	0.002	-0.05279
D5	0.61	0.5262

The material properties of Dyneema and BMG employed are shown in Table 2 below;

Table 2: Material Properties of Dyneema and BMG (Adamant, 2022; Dyneema-Avient, 2019)

Description (Dyneema)	Value	Description (BMG)	Value
Density	975 Kg/m^3	**Density**	6800 Kg/m^3
Axial tensile strength	3.6 x 10^9 N/m^2	**Hardness (Rockwell) (Vickers)**	47 460
Axial tensile modulus	116 x 10^9 N/m^2	**Charpy Impact**	3.5 J/m^2
Axial compressive strength	0.1 x 10^9 N/m^2	**Fatigue Strength**	206 Mpa @ 10^7 Cycles
Axial compressive modulus	116 x 10^9 N/m^2	**Poisson's ratio**	0.38
Transverse tensile strength	0.03 x 10^9 N/m^2	**Young's modulus**	85 x 10^9 N/m^2
Transverse modulus	3 x 10^9 N/m^2	**Ultimate tensile Strength**	1200 x 10^6 N/m^2
Transverse compressive strength	0.1 x 10^9 N/m^2	**Elastic strain (% of original shape)**	1.6 %
		Glass transition temperature	~425 ^{o}C

2.1 Methods

2.1.1 Model Development

The design featured a rectangular shape measuring 120 × 120 mm with a thickness of 9 mm, distributed in a ratio of 4:2:3 mm. During testing, the target material was exposed to impacts from projectiles with blunt and ogival nose shapes traveling at velocities of 215, 249, 264, and 275 m/s.

The target structure comprised three layers: a front layer of Mild steel, a Bulk metallic glass layer sandwiched between the Mild steel and Dyneema laminates, as illustrated in Figure 1. The armor plate design was subjected to fully clamped boundary conditions at all four edges.

To predict the behavior of the Mild steel, the Johnson-Cook plasticity model was utilized. Additionally, the Hashin damage model was employed to forecast the damage of the Dyneema fiber composite.

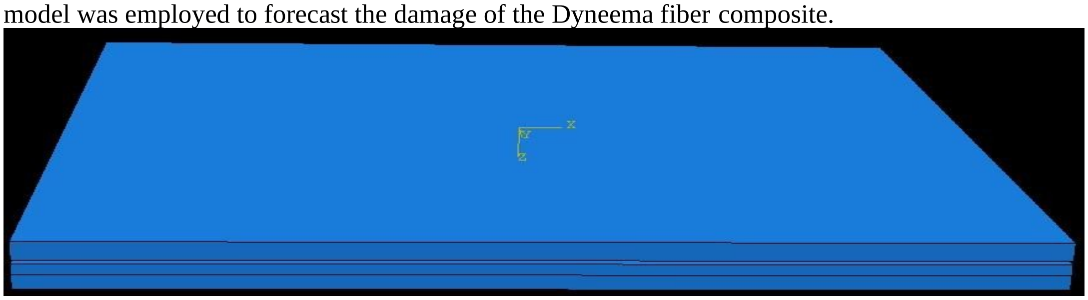

Figure 1: Mild steel, BMG and Dyneema Laminate

The 7.62 mm APM2 projectile comprises a very hard steel core, a gliding metal jacket, a lead nose element, and a lead base filler (Guodong *et al*., 2020). For this study, both a conical-nosed and a blunt-nosed projectile were utilized, depicted in Figures 3 and 4, respectively. The geometry and mass of the projectiles align with the steel core of the 7.62 mm APM2 projectile, as depicted in Figure 2. The material composition was assumed to be hardened 4340 steel.

Meshing of the projectiles was performed using eight-node hexahedral elements (C3D8R). To characterize the material behavior of the projectiles, the Johnson-Cook plasticity model was employed. This model is chosen for its ability to predict the material response of metallic materials under high strain rates experienced during high-velocity impacts (Guodong *et al*., 2020).

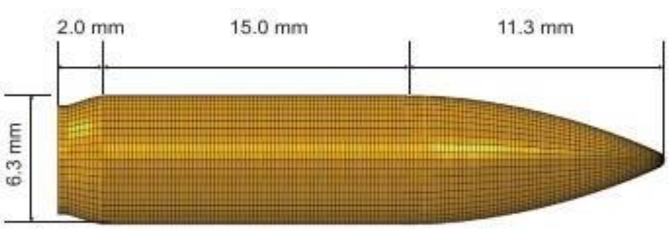

Figure 2: Model of the Conical Projectile and Dimensions

The contact between the projectiles and the target was simulated using the Kinematic contact algorithm. The projectiles were designated as the master entities, while the contact surface of the target served as the slave surface. Hard contact was defined in the normal direction, while a friction coefficient of 0.3 was applied in the tangential direction. The projectiles were discretized using hexahedral elements of constant size, specifically set at 0.0005.

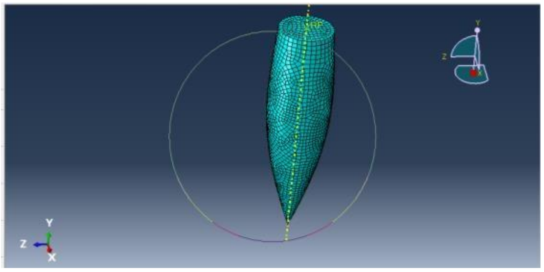

Figure 3: Meshed Conical Projectile

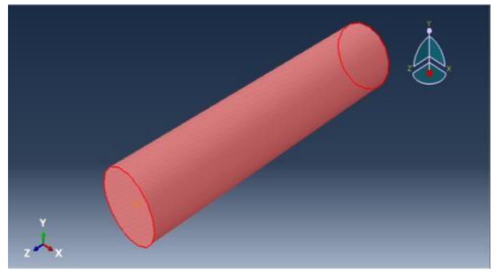

Figure 4: Blunt Projectile

3.0 Results and Discussions

3.1 Results

The result of projectile shape effects using blunt and ogival shapes are summarized in Table 3 and discussed below.

3.2 Discussions

From Table 3 and Figure 5, the results indicate that the Von Mises stresses generated in the target material vary significantly depending on the shape of the projectile and its velocity. The Von Mises stress is an important indicator of the material's deformation and failure under load, making it a crucial parameter to consider in the design and assessment of ballistic protection systems.

Effect of Projectile Shape on Von Mises Stress

The conical projectile consistently generated higher Von Mises stress values compared to the blunt projectile at all tested velocities.

This difference in stress levels can be attributed to the piercing action of the conical projectile, which concentrates the impact force over a smaller area of the target compared to the blunt projectile.

The piercing action of the conical projectile induces localized plastic strain and petal-like formations in the target material, resulting in higher stress concentrations.

Failure Mode for Blunt Nose Projectile

When a blunt nose projectile impacts the target, it initiates a process of high-speed cutting due to shearing forces. The projectile shears out a circular plug from the target material, with a diameter equal to that of the projectile (see Figure 6). This shearing action induces significant plastic deformation in the target material, resulting in the ejection of the plug.

The failure mode associated with blunt nose projectiles is characterized by the formation of a circular plug and the subsequent ejection from the target material.

Failure Mode for Conical Projectile

In contrast to blunt nose projectiles, conical projectiles induce a different failure mode upon impact with the target.

The conical shape of the projectile facilitates piercing of the target material, rather than shearing like the blunt nose projectile. Upon impact, the conical projectile pierces the target, initiating a process known as petalling (see Figure 7). Petalling refers to the formation of radial necking in the target material, where localized plastic strain occurs at the ends of the "petals" created by the piercing action. This radial necking phenomenon is a result of the concentrated force exerted by the conical projectile, leading to deformation and failure of the target material along radial lines from the point of impact.

The failure mode associated with conical projectiles is characterized by the formation of petal-like structures and radial necking in the target material.

Implications of the Results

Higher Von Mises stresses indicate greater deformation and potential failure of the target material. Therefore, the findings suggest that the conical projectile poses a greater threat to the integrity of ballistic protection systems compared to the blunt projectile.

Understanding the stress distribution and failure mechanisms associated with different projectile shapes is crucial for optimizing the design of protective systems. Engineers and designers can use this information to develop more effective armor materials and configurations to enhance protection against specific types of projectiles.

The observed trend in stress distribution is consistent with previous research, validating the reliability and reproducibility of the findings. This reinforces the importance of considering projectile geometry in the design and evaluation of ballistic protection systems (Kpeyingba *et al*., 2013; Senthil *et al*., 2017b; Naik *et al*., 2024).

Table 3: Von Mises Stress Comparison of Conical and Blunt Projectile on Target

S/No.	Velocity (m/s)	Von Mises Stress (N/m^2) for Conical Projectile	Von Mises Stress (N/m^2) for Blunt Projectile
1	275	1.05×10^9	8.647×10^8
2	264	9.5×10^8	8.214×10^8
3	249	8.5045×10^8	6.012×10^8
4	215	7.1685×10^8	3.197×10^8

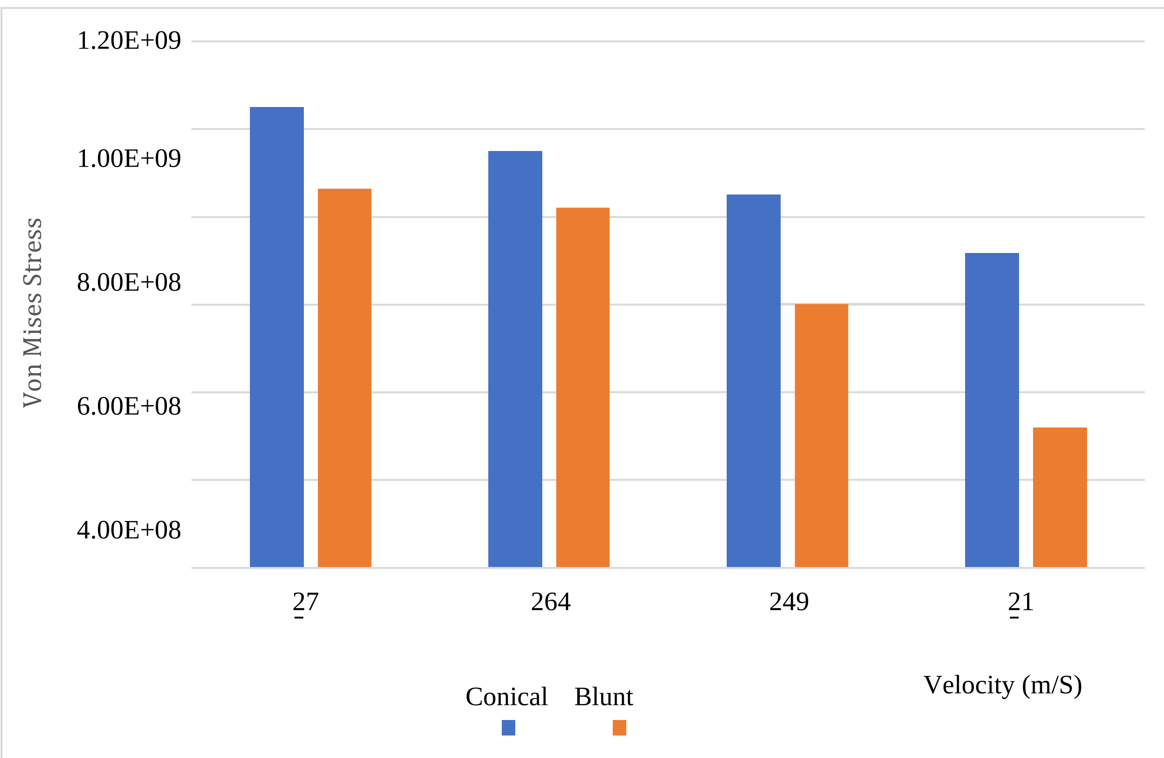

Figure 5: Chart of Von Mises Stress Comparison between Conical and Blunt Projectile

Figure 6: Circular Plug Ejection of Blunt Projectile

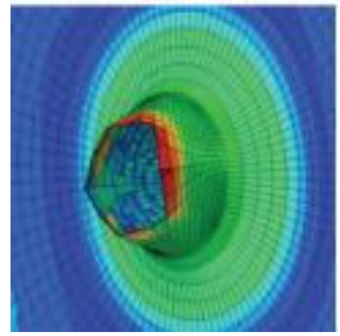

Figure 7: Petal Formation in Target

4.0. Conclusion

In examining the influence of projectile shape on the ballistic performance of laminate composite materials, this study contrasted the effects of blunt and conical projectiles. Employing computational analysis with Abaqus Explicit FEA software, the research focused on mild steel, Bulk metallic glass, and Dyneema, crucial components of modern protective systems, against a conical 7.62 mm API projectile and its blunt counterpart.

The investigation revealed a consistent trend across different velocities, with the conical projectile inducing significantly higher Von Mises stresses compared to the blunt projectile. This disparity in stress distribution stemmed from the piercing action of the conical projectile, leading to localized plastic strain and the formation of petal-like structures. In contrast, the blunt projectile exhibited shearing behavior, resulting in plug ejection events. The implications of these findings underscore the importance of considering projectile shape in the design and optimization of ballistic protection systems. Specifically, tailored design strategies are necessary to accommodate the heightened stress levels induced by conical projectiles.

5.0 Recommendation

Moving forward, future research directions include investigating the effects of hemispherical-shaped projectiles, exploring the cumulative effects of multiple impacts, incorporating dynamic response analysis, and expanding the study to encompass a wider array of laminate composite materials with variations in composition, layering techniques, and thicknesses. These avenues hold promise for further advancing our understanding of the interaction between projectiles and laminate composite materials in ballistic protection applications.

References

Adamant Namiki Precision Jewel Company Limited. 2022. Retrieved February 17, 2022, from https://www.ad-na.com/en/product/jewel/material/bmg.htm

Akindapo, J. O., Orueri, D. U., Johnson-Anamemena, N., and Gideon, C. J. 2023. Modeling and Simulation of Laminate Composite Materials for use as Ballistic Protection. Academy Journal of Science and Engineering. 17(1): 1-19.

Guodong, G., Shah, A., & Larry, D. P. 2020. Numerical Analysis of Ballistic Impact Performance of Two Ceramic-Based Armour Structures. Composites Part C: Open Access, 3, 100061.

Khaire, N., Tiwari, G., and Gurusankar, A. 2020. Numerical Study of Energy Absorption Behaviour of Thin Aluminium Hemispherical Shell against Projectile Impact. Materials Today Proceedings. 21(5): 1958-1963. doi: 10.1016/j.matpr.2020.01.281.

Kpenyigba, M., Tomasz, J., Alexis, R., & Raphael, P. 2013. Influence of Projectile Shape on Dynamic Behaviour Steel Sheet Subjected to Impact and Perforation: Thin-Walled Structures. Elsevier, 93-104.

Kristoffersen, M., Costas, M., Koenis, T., Brotan, V., Paulsen, C. O., and Borvik, T. 2020. On the Ballistic Perforation Resistance of Additive Manufactured AlSi10Mg Aluminium Plates. International Journal of Impact Engineering. 137, 103476. doi: 10.1016/j.ijimpeng.2019.103476.

Naik, M., Pranay, V., Thakur, D. G., Chandel, S., Salunke, S., Pagac, M., and Abouel-Nasr, E. S. 2024. Numerical Investigation on Effect of Different Projectile Nose Shapes on Ballistic Impact of Additively Manufactured AlSi10Mg Alloy. Frontiers in Materials. doi: 10.3389/fmats.2024.1330597.

Nirmal, R. R., Patnaik, B. S., and Jayaganthan, R. 2021. FEM Simulation of High-speed Impact Behaviour of Additively Manufactured AlSi10Mg Alloy. Journal of Dynamic Behaviour of Materials. 7, 469-484. doi: 10.1007/s40870-020-00285-1.

Oktay, K. A., Hafizoglu, H., and Babacan, N. 2022. Effect of Unit Cell Height on the Ballistic Performance of the Body-centered Lattice Structures. International Journal of Innovative Engineering Application. 6(1). 30- 44.

Orueri, D. U., Akindapo, J. O., Johnson-Anamemena, N., and Gideon, C. J. 2023. Characterization of Laminate Composite Materials for Ballistic Protection using Computational Techniques. Nigerian Journal of Engineering Science and Technology Research, vol. 9, No. 2, pp. 31-45.

Orueri, D. U. 2023. Modeling and Simulation of Laminate Composite Materials (Mild Steel-Bulk Metallic Glass-Dyneema) for use as Ballistic Protection (PhD Thesis). Nigerian Defence Academy, Department of Mechanical Engineering.

Senthil, K., Iqbal, M. A., & Gupta, N. K. 2017a. Ballistic Resistance of Mild Steel Plates of Various Thicknesses against 7.62 AP Projectiles. International Journal of Protective Structures, 1-22.

Senthil, K., Iqbal, M. A., & Gupta, N. K. 2017b. Finite Element Studies on Metal Plates against Oblique Impact of Cylindro-Conical Projectiles. In 8th International Conference on Structural Engineering and Construction Management.

Senthil, K., Iqbal, M. A., Arindam, B., Mittal, R., and Gupta, N. K. 2017c. Ballistic Resistance of 2024 Aluminium Plates against Blunt Nose Projectiles. Procedia Engineering, 173, 363-368. doi: 10.1016/j.proeng.2016.12.030.

Tiwari, G., Iqbal, M. A., and Gupta, P. 2017. Influence of Target Span and Boundary Conditions on Ballistic Limit of Thin Aluminium Plate. Procedia Engineering. 173. 169-174.

Yang, Y., and Chen, X. 2017. Investigation of Failure Modes and Influence on Ballistic Performance of Ultra-High Molecular Weight Polyethylene (UHMWPE) Uni-directional Laminate for Hybrid Design. Composite Structures. doi: https://doi.org/10.1016/j.compstruct.2017.04.033